Supporting Information

Improving peroxymonosulfate activation by copper ions saturated adsorbent-based single atom catalysts for organic contaminants degradation: Electron-transfer mechanism and key role of Cu single-atoms

Jingwen Pan, Baoyu Gao*, Pijun Duan, Kangying Guo, Muhammad Akram, Xing Xu, Qinyan Yue, Yue Gao**

Shandong Key Laboratory of Water Pollution Control and Resource Reuse, School of Environmental Science and Engineering, Shandong University, Qingdao 266237, PR China

Text: 4; Figure: 13; Table: 5.

*Corresponding author: E-mail: bygao@sdu.edu.cn (B. Y. Gao)

** Corresponding author: E-mail: gaoyue0322@aliyun.com (Y. Gao)

Text S1 Fabrication of Cu@NBC/PSF membrane

The 15 mg of 3SACu@NBC powders were deposited on PSF membranes by direct filtration of 3SACu@NBC suspension liquid and heated at 60 ^{o}C for 2 h. The effective membrane area was 49 cm^2. The membranes should be prewetted with deionized water before using, and placed in the dead-end ultrafiltration cell. At a predetermined time, the effluent was collected to quantify the pollutant removal efficiency.

Text S2 Characterization

Xray diffraction (XRD) patterns were acquired on an X-ray powder di□raction (XRD, Rigaku Ultima IV, Japan). X-ray photoelectron spectroscopy (XPS) of samples were analyzed using Multifunctional imaging electron spectrometer (Thermo ESCALAB 250XI, US). The surface areas (SA) of Cu-Fe@BRC was recorded on a Micrometrics Tristar 3000 using the Brunauer-Emmett-Teller (BET) N_2 adsorption-desorption method. X-ray absorption spectroscopy (XAS) of Cu edge was performed on Taiwan Synchrotron Irradiation Facility with stored electron energy of 3 GeV to obtain fine structure information of SACu@NBC. High-angle annular dark-field scanning transmission electron microscopy (HAADF-STEM) were carried out on FEI Theims Z, Titan Cubed Themis G2300. Cu content in SACu@NBC was characterized by ICP-OES (Agilent 5110). Electron paramagnetic resonance (EPR) spectrometer (Bruker A300, Germany) was employed to probe the radicals generated in PMS activation process. In-situ Roman was performed on Thermo DXR3xi Raman Imaging Microscope. The degradation intermediates were identified by a high-performance liquid chromatography-mass spectrometry (HPLC-MS, maXis, Bruker Co., USA).

Text S3 Electrochemical measurement.

CV was performed between – 0.1 V and + 1.0 V at a scan rate of 10 mV s^{-1} using an electrochemical workstation. The experiments were conducted in 20 mM phosphate buffer solution (PBS) and 0.05 mM PCs with a three-electrode-cell configuration including a working electrode (20×20×1 mm of graphite plate), a counter electrode (platinum electrode), and a reference electrode (saturated calomel electrode, SCE). Half-wave potentials ($\varphi_{1/2}$) were calculated by eq. S1 and eq. S2 in the irreversible and reversible systems, respectively:

$$\varphi_{1/2} = \frac{1}{2}(E_p + E_{p/2}) \quad \text{S1}$$

where E_p and $E_{p/2}$ are the peak potential and half-peak potential (potential of half the peak current), respectively.

$$\varphi_{1/2} = \frac{1}{2}(E_{pa} + E_{pc}) \quad \text{S2}$$

where Epa and Epc are anodic peak potential and cathodic peak potential, respectively.

Open circuit potential was monitored by chronopotentiometry analysis, which were conducted at room temperature in a standard three-electrode electrochemical cell with an Ag/AgCl (4 M KCl) reference electrode, a platinum wire counter electrode and a catalyst-modified glassy carbon working electrode (0.196 cm^2, Pine Research Instrumentation, USA). The system can also measure the potential variations at the electrode with the addition of PMS or/and BPA with 20 mM boratory buffer solution as supporting electrolyte.

Text S4 Density functional theory (DFT) calculation.

Density functional theory calculations are performed using the projector augmented wave method and a plane-wave basis set as implemented in the Vienna ab-initio simulation package. The Perdew-Burke-Ernzerhof functional for the exchange-correlation term is used for all calculations. The energy cutoff for the plane wave basis set is set to be 400 eV. The lattice constant of N-doped graphene with or without Cu is constructed to be a=12.30 Å and b =12.30 Å. The vacuum thickness is set to be 15 Å along the z direction. A Monkhorst-Pack (3×3×1) k-point is used to sample the Brillouin zone. The electronic energy was considered self-consistent when the energy change was smaller than 10^{-6} eV. The supercell box is fixed and all atoms are allowed to fully relax until the residual force per atom is less than 0.01 eV $Å^{-1}$.

The formation energy (E_{form}) [1] of an Cu atom on N-doped graphene was defined as：

$$E_{form} = E_{Cu\text{-}surf} - E_{surf} - E_{Cu} \quad \text{S3}$$

where $E_{Cu\text{-}surf}$ and E_{surf} are the energy of the N-doped graphene with Cu atom and without Cu atom, and the E_{Cu} are the energy of a Cu atom in bulk Cu structure.

The adsorption energy (E_{ads}) [2] of an adsorbate HSO_5^- was defined as：

$$E_{ads} = E_{HSO5\text{-}/surf} - E_{surf} - E_{HSO5\text{-}} \quad \text{S4}$$

where $E_{HSO5\text{-}/surf}$, E_{surf} and $E_{HSO5\text{-}}$ are the energy of HSO_5^- adsorbed on the surface, the energy of the clean surface, and the energy of HSO_5- in a 15x15x15 $Å^3$ box, respectively.

Fig. S1 The Morphology photo of catalyst after pyrolysis.

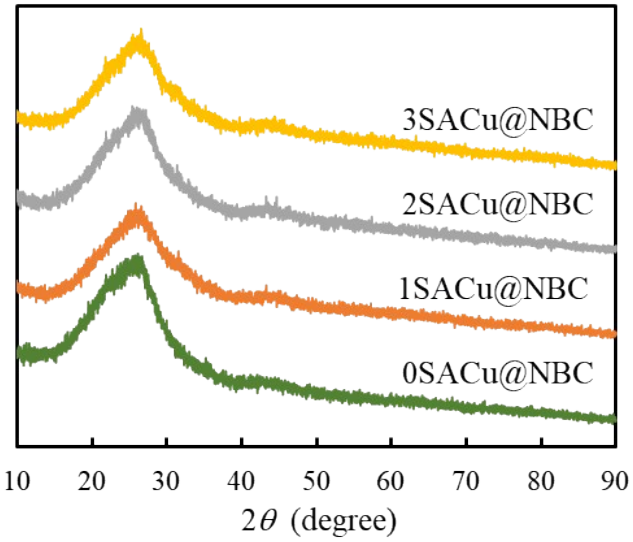

Fig. S2 Wide-angle XRD patterns for the samples of SACu0@NBC, SACu10@NBC, SACu20@NBC and SACu30@NBC.

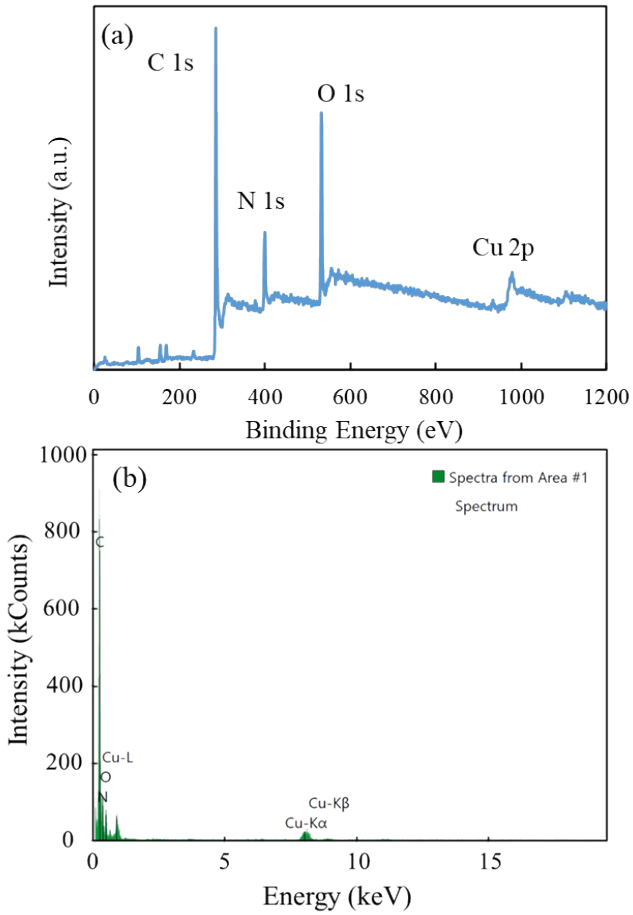

Fig. S3 (a) Full scan XPS spectra and (b) EDX spectrum of 3SACu@NBC.

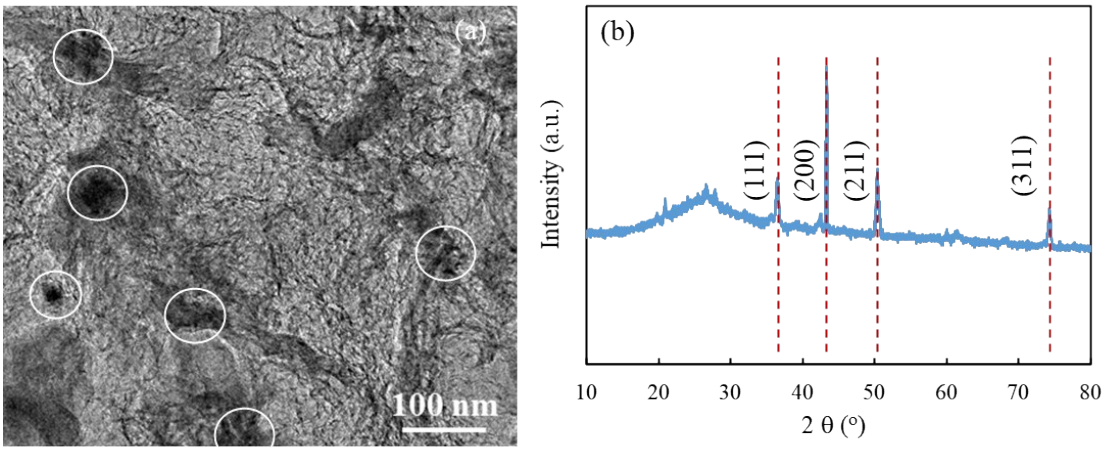

Fig. S4 The TEM image and wide-angle XRD pattern of the Cu@BC.

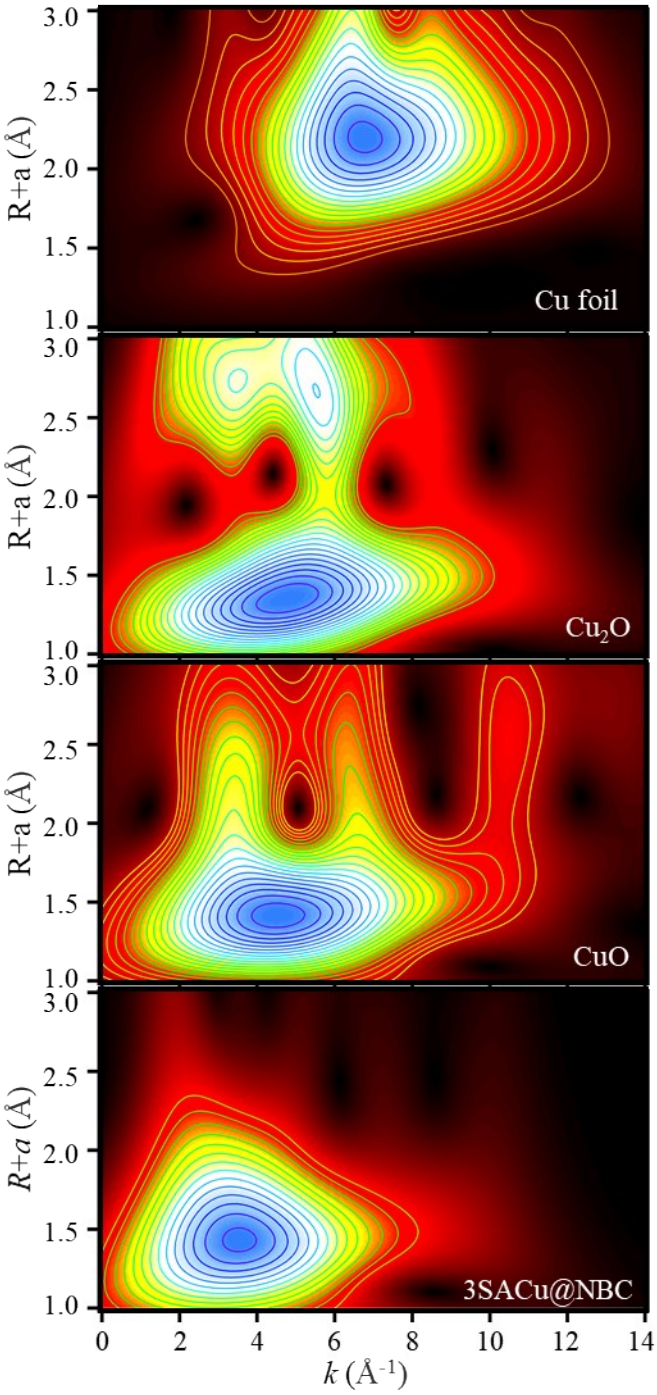

Fig. S5 WT plot of 3SACu@NBC.

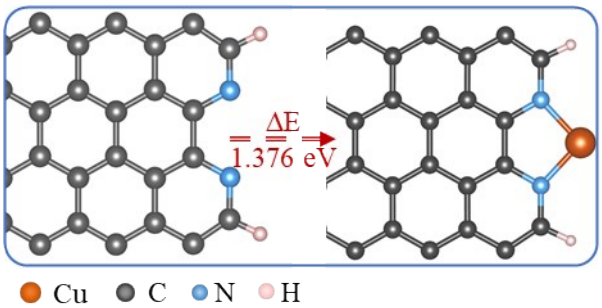

Fig. S6 The formation energies of Cu-N_2.

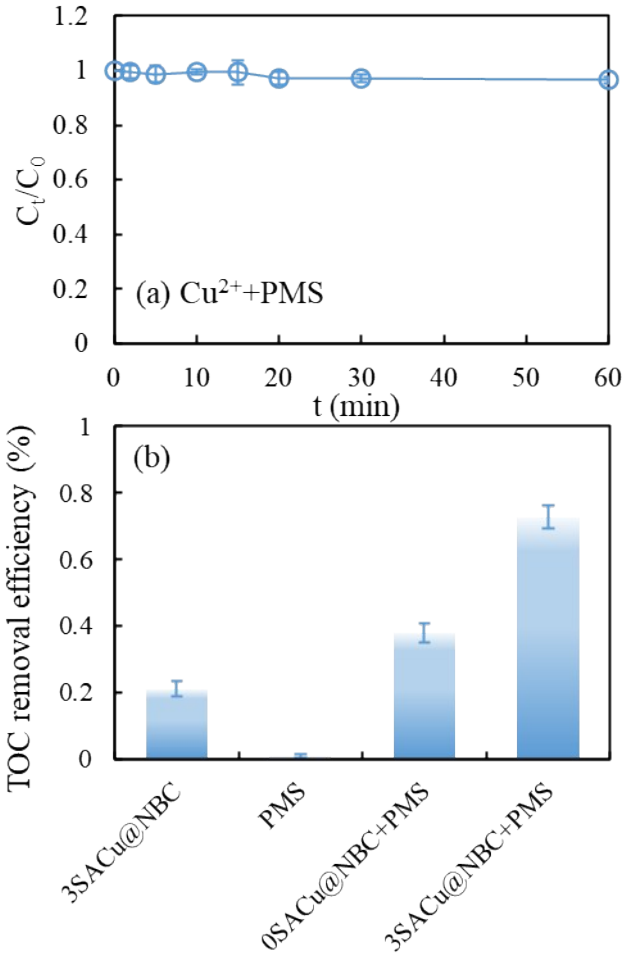

Fig. S7 (a) BPA removal in Cu^{2+}/PMS system ([Cu^{2+}] = 0.01 mg/L, [BPA] = 20 mg/L, [PMS] = 0.4 g/L, T = 25 °C); (b) TOC removal efficiencies during BPA degradation in different system ([catalysts] = 0.1 g/L, [BPA] = 20 mg/L, [PMS] = 0.4 g/L, T = 25 °C, pH=7).

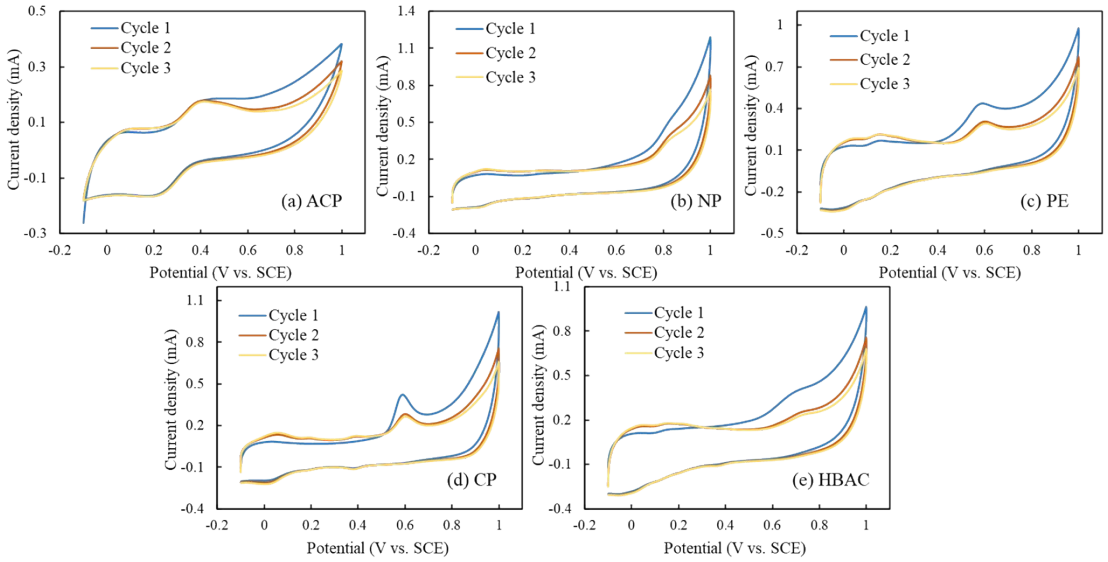

Fig. S8 CV curves on the graphite electrodes in (a) ACP, (b) NP, (c)PE, (d) CP and (d) HBAC solutions. ([organics]$_0$ = 0.05 mM, [PBS] = 20 mM).

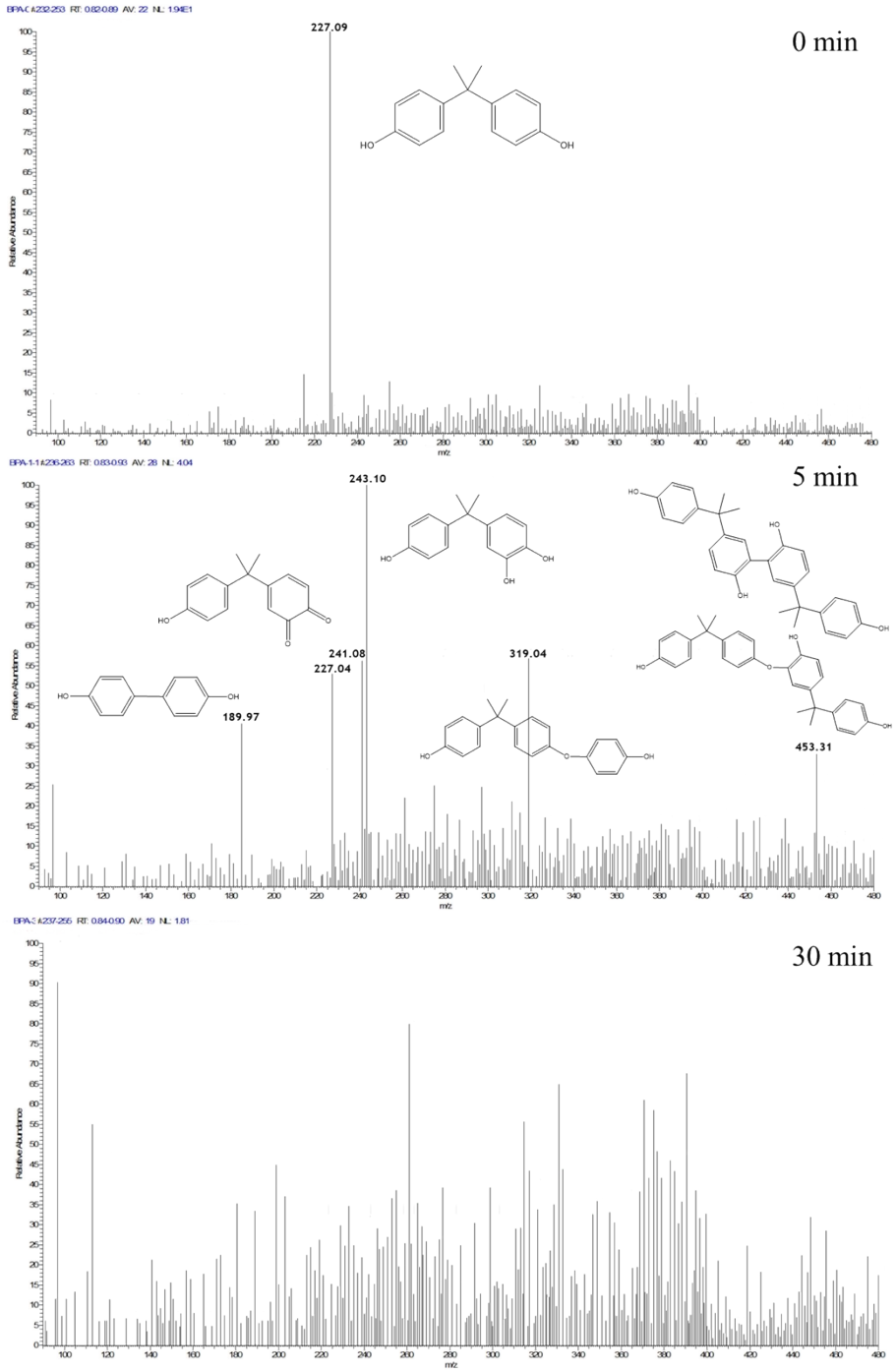

Fig. S9 LC-MS of BPA and intermediates in 3SACu@NBC/PMS system at different time.

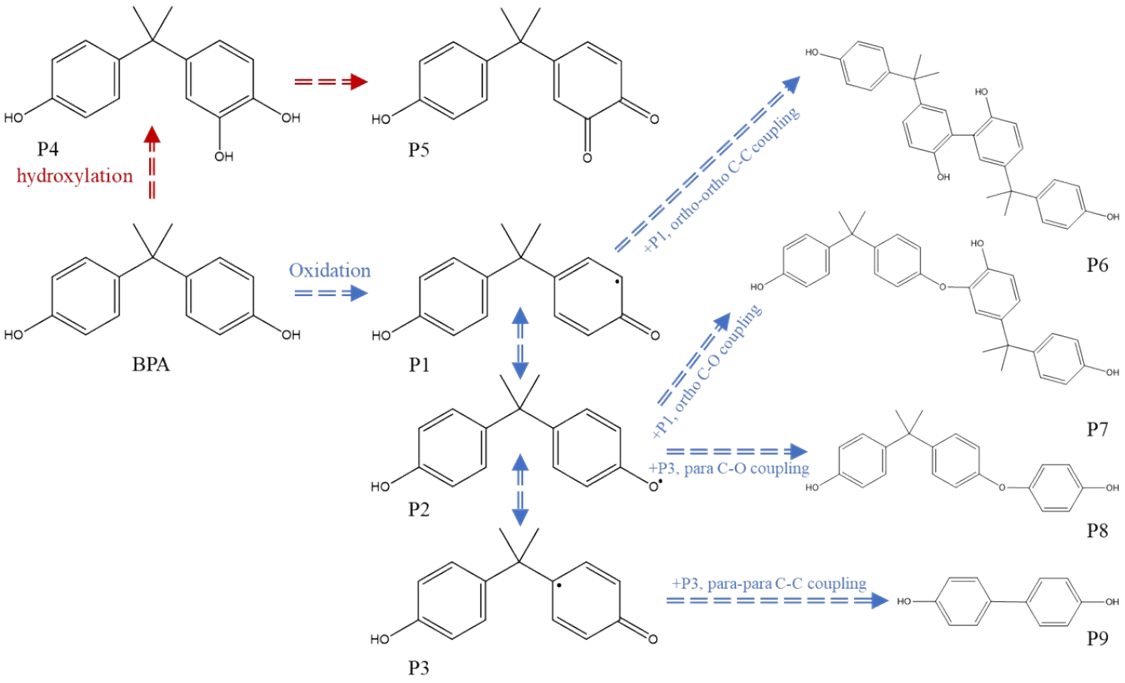

Fig. S10 Proposed transformation pathways of BPA in 3SACu@NBC/PMS system.

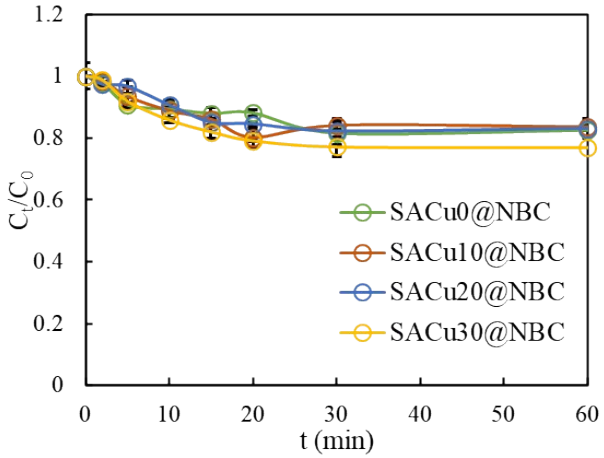

Fig. S11 BPA adsorption by different SACu@NBC catalysts ([SACu@NBC]=0.1 g/L, [PMS]=0.4 g/L, $[BPA]_0$=20 mg/L, T=25 °C, and pH=7.0).

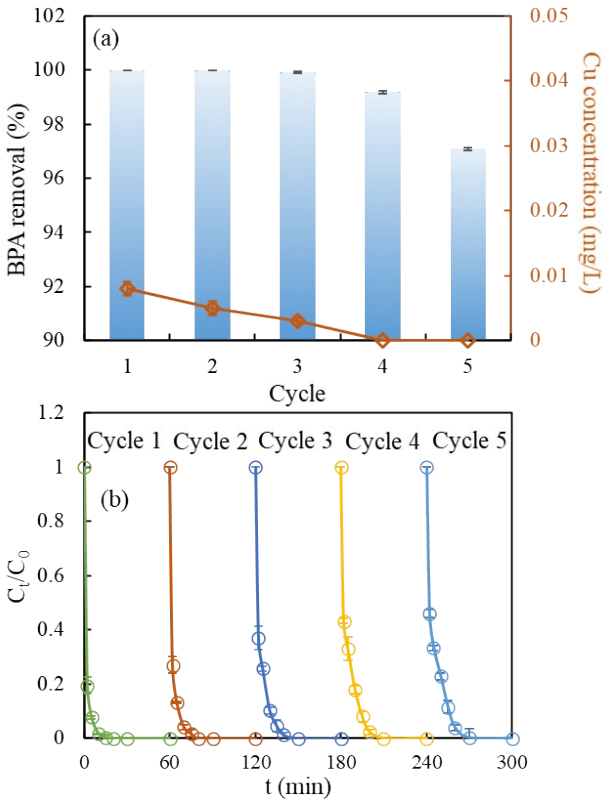

Fig. S12 Catalyst recyclability of 3SACu@NBC ([PMS]=0.4 g/L, $[BPA]_0$=20 mg/L, T=25 °C, and pH=7.0).

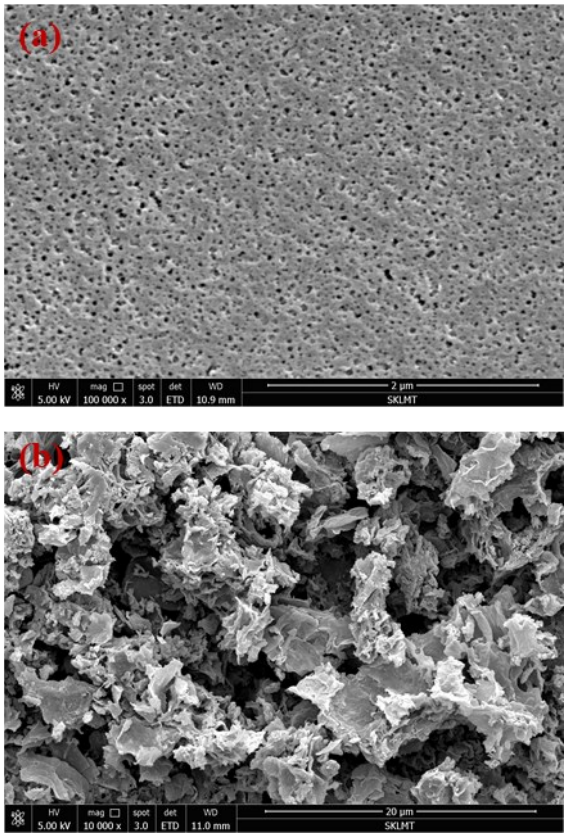

Fig. S13 Scanning electron microscope (SEM) images of the top-sections of (a) PSF and (b) SACu@NBC/PSF membrane.

Table S1. EXAFS fitting parameters at the Cu K-edge for various samples (S_0^2=0.8)

Sample	Shell	N	ΔE (eV)	R (Å)	σ^2 (Å^2)	R-factor
Cu foil	Cu-Cu	12	3.60±0.58	2.538±0.003	0.00848±0.0005	0.004
Cu_2O	Cu-O	2	6.24±1.23	1.852±0.0515	0.00508±0.0023	0.006
	Cu-Cu	12	6.24±1.23	3.023±0.0842	0.0114±0.0023	
CuO	Cu-O	4	2.23±0.26	1.943±0.013	0.0040±0.0012	0.012
3SACu@NBC	Cu-N	4.26±0.16	4.73±0.46	1.923±0.003	0.0111±0.0008	0.0006

Note: N: coordination number; ΔE: the edge-energy shift; R: the internal atomic distance; σ^2: Debye–Waller factor.

Table S2. Specific HPLC conditions for different organic compounds.

Chemical	Mobile phase		Flow rate /mL min^{-1}	Wavelength /nm
	Methanol /%	Water /%[a]		
Bisphenol A	70	30	1.0	280
Phenol	50	50	1.0	270
4-chlorophenol	70	30	1.0	280
4-nitrophenol	70	30	1.0	280
Acetaminophen	20	80	1.0	243
4-hydroxybenzoic acid	70	30	0.9	254

[a] 1% acetic acid

Table S3. The catalytic performance comparison in complete BPA degradation.

Catalyst	BPA concentration	Catalyst dosage	Oxidant dosage	Time	Ref
NGC 700	20 mg/L	0.1 g/L	PMS, 0.2 g/L	6 min	3
NBC-1000	5 mg/L	0.2 g/L	PMS, 0.3 g/L	>60 min	4
Fe@CNs	20 mg/L	0.1 g/L	PDS, 0.5 mM	60 min	5
Fe_{SA}-N-C-20	20 mg/L	0.15 g/L	PMS, 0.4 g/L	30 min	6
$La_2CuO_{4-\delta}$	0.05 mM	0.5 g/L	PMS, 2 mM	60 min	7
Cu@NBC	10 mg/L	0.1 g/L	PDS, 0.2 g/L	60 min	8
SACu@NBC	20 mg/L	0.1 g/L	PMS, 0.4 g/L	30 min	This work

Table S4. Band gaps of NBC and 3SACu@NBC.

Sample	Band gap (eV)
NBC	0.451
SACu@NBC	0.282

Table S5 Characteristics of simulated simulate polycarbonate wastewater treatment.

Parameter	Value	Unit
BPA (Bisphenol A)	50	mg/L
COD (Chemical oxygen demand)	293.4 ± 38	mg/L
TOC (Total organic carbon)	111.3 ± 15	mg/L
HCO_3^- (Bicarbonate)	10000	mg/L
Cl^- (Chlorides)	14000	mg/L
Conductivity	30300 ± 230	µS/cm
pH (25 ^oC)	8.0 ± 0.2	–
Turbidity	20.2 ± 2	NTU
Appearance	tawny	–

Reference

1. W. Li, X. Li, J. Yu, J. Liao, B. Zhao, L. Huang, A. Ali, H. Zhang, J. H. Wang, Z. Guo and M. Liu, *Nano Energy*, 2019, **61**, 594-603.
2. C. Chen, T. Ma, Y. Shang, B. Gao, B. Jin, H. Dan, Q. Li, Q. Yue, Y. Li, Y. Wang and X. Xu, *Appl. Catal., B*, 2019, **250**, 382-395.
3. R. Luo, M. Li, C. Wang, M. Zhang, M. A. Nasir Khan, X. Sun, J. Shen, W. Han, L. Wang and J. Li, *Water Res.*, 2019, **148**, 416-424.
4. W.-D. Oh, G. Lisak, R. D. Webster, Y.-N. Liang, A. Veksha, A. Giannis, J. G. S. Moo, J.-W. Lim and T.-T. Lim, *Appl. Catal., B*, 2018, **233**, 120-129.
5. L. Liu, X. Xu, Y. Li, R. Su, Q. Li, W. Zhou, B. Gao and Q. Yue, *Chem. Eng. J.*, 2020, **382**.
6. Y. Li, T. Yang, S. Qiu, W. Lin, J. Yan, S. Fan and Q. Zhou, *Chem. Eng. J.*, 2020, **389**.
7. H. Chen, Y. Xu, K. Zhu and H. Zhang, *Appl. Catal., B*, 2021, **284**.
8. J. Pan, B. Gao, Y. Gao, P. Duan, K. Guo, M. Akram, X. Xu and Q. Yue, *Chem. Eng. J.*, 2021, DOI: 10.1016/j.cej.2021.129441.